Propagation of Elastic-Plastic Stress Waves under Plane Strain

Kouji FUKATSU and Ikuyoshi IIDA
Department of Mechanical Engineering

(Received September 9, 1975)

Summary

This paper deals with the problem of propagation of two-dimensional waves through a strain rate-sensitive and elastic-plastic rectangular plate, which has four boundaries. The propagation is governed by a quasi-linear hyperbolic partial differential equation, which has three independent variables. The solutions of this differential equation are obtained by solving the finite difference equations by integration along bicharacteristics.

This procedure of solution has enabled to obtain numerical solutions of dynamic boundary-value problem.

The theoretical results in this paper show that unloading regions are produced near the center of the symmetric surface because of reflection of waves from the free boundaries and that the place where the shearing stress is the largest hardly changes during the application of impulsive load.

1. Introduction

The theoretical study of elastic-plastic stress waves in a rectanguler plate under conditions of plane strain is made. This paper deals with the problem of a rectangular plate of which one edge is loaded by an arbitrary normal pressure $P(x,t)$. The influence of the reflection from the free boundary and fixed end on the disturbance propagating in the plate is considered. A Malvern type constitutive equation is adopted and the analyzation of two-dimension elastic-plastic waves in a half-space by Bejda[1] is applied.

Since dynamic plasticity was studied in 1940, its investigations have been widely applied to the problems of high-velocity impact and forming of metals and to the elucidation of the destructible mechanism caused by an earthquake. At first the waves in a bar were analyzed.[2),3)] Thereafter axisymmetric waves[4)] originating from a cylindrical hole in a plate, simple waves[5),6)] in a half space and the combined waves[7)] which are propagated in thin-walled tubes were analyzed. As all these analyses are one dimensional problems, they may not sufficiently explaine the real phenomena. In order to supply their imperfectness, in recent years much attension has been devoted to the analyses of propagation of two-dimensional stress waves.

In the case of a half-space this problem has been analyzed by Bejda.[1)] The governing equations form a system of quasi-linear hyperbolic partial differential equation in three independent variables. The solutions are obtained using finite difference equations deduced by integration along bicharacteristics.

In this paper the applicability of this method to a finite space is verified and the propagation of the stress waves in the plate is explanated.

2. Derivation of the general equations

Consider a material finite to x- and y-direction and semi-infinite to z- direction in the Cartesian system of coordinates x, y, z. At time $t=0$ an arbitrary pressure $P(x,t)$ is applied on the plane $y=0$ (Fig.1). The constitutive equations for elastic-plastic material are assumed to have the following form.

$$\dot{\varepsilon}_{ij}=\dot{S}_{ij}/(2G)+\delta_{ij}\dot{\sigma}_m/(3K)+S_{ij}\Phi(\bar{\sigma},\bar{\varepsilon}_p) \qquad (1)$$

where the non-instantaneous plastic response term Φ

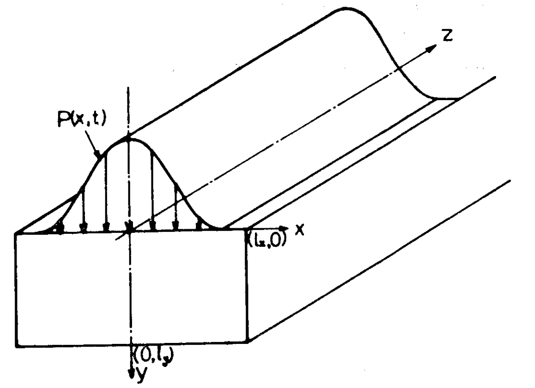

Fig. 1 Distribution of the pressure $P(x, t)$ on the boundary $y=0$.

is

$$\Phi=\frac{\bar{\sigma}-f(\bar{\varepsilon}_p)}{\bar{\sigma}}$$

ε_{ij} : components of the strain tensors

S_{ij} : components of the deviatoric stress tensors

$\bar{\sigma}$: equivalent stress

$\bar{\varepsilon}_p$: equivalent plastic strain

$f(\bar{\varepsilon}_p)$: quasi-static plastic stress-strain relation.

The dot denotes differentiation with respect to time and K, G, σ_m are bulk modulus, stiffness modulus. mean stress, respectively. Assuming the plane strain conditions the constitutive Eqs.(1) now becomes:

$$\frac{\partial v_x}{\partial x}=\frac{1}{2G}\dot{S}_x+\frac{1}{3K}\dot{\sigma}_m+S_x\Phi(\bar{\sigma},\bar{\varepsilon}_p) \quad (2a)$$

$$\frac{\partial v_y}{\partial x}=\frac{1}{2G}\dot{S}_y+\frac{1}{3K}\dot{\sigma}_m+S_y\Phi(\bar{\sigma},\bar{\varepsilon}_p) \quad (2b)$$

$$0=\frac{1}{2G}\dot{S}_z+\frac{1}{3K}\dot{\sigma}_m+S_z\Phi(\bar{\sigma},\bar{\varepsilon}_p) \quad (2c)$$

$$\frac{\partial v_x}{\partial y}-\frac{\partial v_y}{\partial x}=\frac{1}{G}\dot{\tau}+2\tau\Phi(\bar{\sigma},\bar{\varepsilon}_p) \quad (2d)$$

where, together with the equations of motion

$$\frac{\partial \sigma_x}{\partial x}+\frac{\partial \tau_{xy}}{\partial y}=\rho\frac{\partial v_x}{\partial t}, \quad (3a)$$

$$\frac{\partial \tau_{xy}}{\partial x}+\frac{\partial \sigma_y}{\partial y}=\rho\frac{\partial v_y}{\partial t}, \quad (3b)$$

where ρ is the density of the material, form the system of equations.

Now to simplify the calculation we introduce the following dimensionless quantities.

$$u=\frac{\hat{v}_x}{c_1},\ v=\frac{\hat{v}_y}{c_1},\ t=\frac{\hat{t}c_1}{b},\ x=\frac{\hat{x}}{b},\ y=\frac{\hat{y}}{b},$$
$$\Gamma=\frac{c_1}{c_2},\ \Phi=b\rho c_1\hat{\Phi},\ p=\frac{\sigma_x+\sigma_y}{\rho c_1^2},\ q=\frac{\sigma_x-\sigma_y}{\rho c_1^2},$$
$$r=\frac{\sigma_z}{\rho c_1^2},\ \tau=\frac{\hat{\tau}}{\rho c_1^2} \quad (4)$$

Here a hat '^' denotes the corresponding dimensional quantity, c_1 and c_2 are the velocity of propagation of elastic dilatational waves and of elastic shear waves, b an arbitrary characteristic length. The speeds c_1 and c_2 are given by

$$c_1=\left(\frac{3K+4G}{3\rho}\right)^{\frac{1}{2}},\ c_2=\left(\frac{G}{\rho}\right)^{\frac{1}{2}} \quad (5)$$

Using the notation described above the general equations can be written as

$$L[\mathrm{W}]=\mathrm{A}^t\mathrm{W}_t+\mathrm{A}^x\mathrm{W}_x+\mathrm{A}^y\mathrm{W}_y-\mathrm{B}=0, \quad (6)$$

where the vectors W, B and tensors A^t, A^x, A^y are:

$$\mathrm{W}=\begin{pmatrix} u\\ v\\ p\\ q\\ r\\ \tau \end{pmatrix}\quad \mathrm{B}=\begin{pmatrix} 0\\ 0\\ -\frac{2}{3}(p-r)\Phi\\ -2q\Phi\\ -\frac{2}{3}(r-p)\Phi\\ -2\tau\Phi \end{pmatrix}\quad \mathrm{A}^t=\begin{pmatrix} 1&0&0&0&0&0\\ 0&1&0&0&0&0\\ 0&0&M&0&Q&0\\ 0&0&0&\Gamma^2&0&0\\ 0&0&Q&0&N&0\\ 0&0&0&0&0&\Gamma^2 \end{pmatrix}$$

$$\mathrm{A}^x=\begin{pmatrix} 0&0&-1&-1&0&0\\ 0&0&0&0&0&-1\\ -1&0&0&0&0&0\\ -1&0&0&0&0&0\\ 0&0&0&0&0&0\\ 0&-1&0&0&0&0 \end{pmatrix}\quad \mathrm{A}^y=\begin{pmatrix} 0&0&0&0&0&-1\\ 0&0&-1&1&0&0\\ 0&-1&0&0&0&0\\ 0&1&0&0&0&0\\ 0&0&0&0&0&0\\ -1&0&0&0&0&0 \end{pmatrix} \quad (7)$$

in which $M=\Gamma^4/(3\Gamma^2-4)$, $N=\Gamma^2(\Gamma^2-1)/(3\Gamma^2-4)$, $Q=\Gamma^2(2-\Gamma^2)/(3\Gamma^2-4)$.

Equations(6) constitute a quasi-linear hyperbolic system of partial differeftial equations.

3. Characteristic properties of the governing equations

The condition that a surface $\phi(x, y, t)=$const. be a characteristic surface of Eqs.(6) is the condition that the determinant of the characteristic matrix A defined by

$$\mathrm{A}=\mathrm{A}^t\phi_t+\mathrm{A}^x\phi_x+\mathrm{A}^y\phi_y \quad (8)$$

be zero. The characteristic equation DetA=0 can be written as

$$\{\phi_t^2-(\phi_x^2+\phi_y^2)\}\{\phi_t^2-(\phi_x^2+\phi_y^2)/\Gamma^2\}\phi_t^2=0. \quad (9)$$

The two terms in-brackets represent the velocities of propagation of elastic dilatational and elastic shear waves. From Eqs.(6) it is clear that the term which represents the plastic behavior is not contained in the analysis of characteristic surface.

The bicharacteristics of Eqs.(6) are the generators of the following characteristic cones passing through the point (t_0, x_0, y_0):

$$c^2(t-t_0)^2=(x-x_0)^2+(y-y_0)^2,\ c=1, 1/\Gamma. \quad (10)$$

It is convenient to introduce the following parametrization of the characteristic cones in terms of the two parameters α and $\tilde{t}$:

$$x-x_0=c\tilde{t}\cos\alpha \qquad c=1,\ 1/\Gamma,$$
$$y-y_0=c\tilde{t}\sin\alpha, \tag{11}$$
$$t-t_0=\tilde{t}.$$

Relations(11) give the disired equations of bicharacteristic cones. The bicharacteristic strips associated with the bicharacteristic lines(11) are:

$$\phi_t=c,\ c=1,\ 1/\Gamma$$
$$\phi_x=-\cos\alpha, \tag{12}$$
$$\phi_y=-\sin\alpha.$$

In order to determine the equations along bicharacteristics, the null vectors associated with the system(6) must first be determined.

The null vectors $1=[l_1,\ l_2,\ l_3,\ l_4,\ l_5,\ l_6]$ are the solutions of the following homogeous system of equations:

$$1\cdot A=0 \tag{13}$$

The solutions of Eqs.(13) are given as following using the Eqs.(8) and (12):

$$1=[-\Gamma^2\cos\alpha,\ -\Gamma^2\sin\alpha,\ \Gamma^2-1,\ \cos2\alpha,\ \Gamma^2-2,\ \sin2\alpha] \tag{14a}$$

for $c=1$, and

$$1=[\Gamma\sin\alpha,\ -\Gamma\cos\alpha,\ 0,\ -\sin2\alpha,\ 0,\ \cos2\alpha] \tag{14b}$$

for $c=1/\Gamma$.

The disired differential equations along bicharacteristics are obtained from the equation

$$1\cdot L[W]=0 \tag{15}$$

From Eqs.(15) the following incremental relations along the characteristics are obtained.

$$\cos\alpha du+\sin\alpha dv+dp+\cos2\alpha dq+\sin2\alpha d\tau = -S_1(\alpha)\,dt$$

for $c=1$, and (16a)

$$-\Gamma\sin\alpha du+\Gamma\cos\alpha dv-\Gamma^2\sin2\alpha dq+\Gamma^2\cos2\alpha d\tau = -S_2(\alpha)\,dt$$

for $c=1/\Gamma$, (16b)

where $S_1(\alpha)$ and $S_2(\alpha)$ are

$$S_1(\alpha)=\left[-\sin^2\alpha+\frac{1}{\Gamma^2}(1-\cos2\alpha)\right]u_x+\left(\frac{1}{2}-\frac{1}{\Gamma^2}\right)(u_y+v_x)\times\sin2\alpha+q_x(\cos2\alpha-1)\cos\alpha+q_y(1+\cos2\alpha)\sin\alpha+\left[-\cos^2\alpha+\frac{1}{\Gamma^2}(1+\cos2\alpha)\right]v_y+(1-2\sin^2\alpha)\times(\tau_x\sin\alpha-\tau_y\cos\alpha)+\frac{2\Phi}{\Gamma^2}\left(\frac{p-r}{3}+q\cos2\alpha+\tau\sin2\alpha\right) \tag{17a}$$

$$S_2(\alpha)=\frac{1}{2}(u_x-u_y)\sin2\alpha-u_y\cos^2\alpha+\Gamma p_x\sin\alpha-\Gamma q_x\sin\alpha\times\cos2\alpha+\Gamma\tau_y(1+\cos2\alpha)\sin\alpha+v_x\sin^2\alpha-\Gamma p_y\times\cos\alpha+\Gamma q_y\cos\alpha\cos2\alpha-\Gamma\tau_x(1-\cos2\alpha)\cos\alpha-2\Phi\times(q\sin2\alpha-\tau\cos2\alpha). \tag{17b}$$

4. Integration scheme

We regard the plane z=cost. as covered by a square mesh with mesh size h. Difference equations are derived for computing the solution at a mesh point (t_0, x_0, y_0) (hereafter called simply 0) from known data at neighboring mesh points on the plane $t=t_0-k$ (see Fig.2). These equations are obtained by forming combinations of equations resulting from integration of Eqs.(16) along the bicharacteristics and integration of Eqs.(6) along the line $x=x_0$, $y=y_0$.

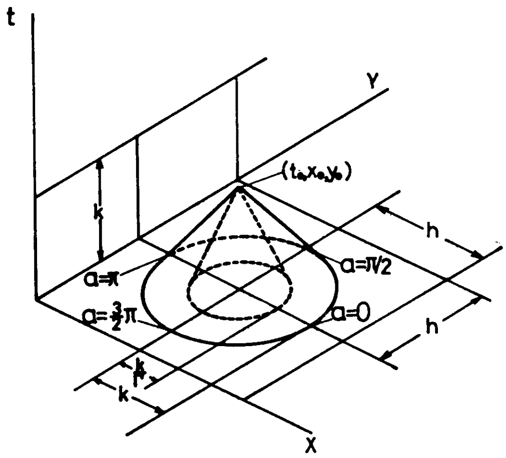

Fig. 2 Characteristic cones for the dynamic elastic, viscoplastic equations.

Integration of Eqs.(16) along the bicharacteristics for which $\alpha=\alpha_i$, from the point 0 to the point of intersection of the bicharacteristic with the plane $t=t_0-k$ gives

$$\cos\alpha_i\delta u+\sin\alpha_i\delta v+\delta p+\cos2\alpha_i\delta q+\sin2\alpha_i\delta\tau = -k[S_1(\alpha_i)^0+S_1(\alpha_i)_i]/2-W_1(\alpha_i) \tag{18a}$$

$$-\Gamma\sin\alpha_i\delta u+\Gamma\cos\alpha_i\delta v-\Gamma^2\sin2\alpha_i\delta q+\Gamma^2\cos2\alpha_i\delta\tau = -k[S_2(\alpha_i)^0+S_2(\alpha_i)_i]/2-W_2(\alpha_i) \tag{18b}$$

for the exterior and interior cones respectively where for example δu denotes the increment $u(t_0, x_0, y_0)-u(t_0-k, x_0, y_0)$ and where

$$W_1(\alpha_i)=\cos\alpha_i(u_0-u_i)+\sin\alpha_i(v_0-v_i)+\cos2\alpha_i(q_0-q_i)+\sin2\alpha_i(\tau_0-\tau_i)+p_0-p_i, \tag{19a}$$

$$W_2(\alpha_i)=-\Gamma\sin\alpha_i(u_0-u_i)+\Gamma\cos\alpha_i(v_0-v_i)-\Gamma^2\sin2\alpha_i\times(q_0-q_i)+\Gamma^2\cos2\alpha_i(\tau_0-\tau_i). \tag{19b}$$

In Eqs.(18) the superscript ^{0} denotes evaluation of the function at the point 0; the subscript $_0$ denotes evaluation of the function at the point (t_0-k, x_0, y_0);

the subscript i denotes evaluation of the function at the point where the bicharacteristic α_i on the appropriate characteristic cone intersects the plane $t=t_0-k$.

Additional equations involving the increments δu, ..., $\delta\tau$ can be obtained by integration of Eqs.(6) along the line $x=x_0$, $y=y_0$ from $t=t_0-k$. Thus they are as follows

$$\delta u=\frac{k}{2}[(p_x+q_x+\tau_y)^0+(p_x+q_x+\tau_y)_0], \quad (20a)$$

$$\delta v=\frac{k}{2}[(p_y-q_y+\tau_x)^0+(p_y-q_y+\tau_x)_0], \quad (20b)$$

$$\delta p=\frac{k}{2}\left[\left(\frac{\Gamma^2-1}{\Gamma^2}(u_x+v_y)-\frac{2\Phi}{3\Gamma^2}(p-r)\right)^0+\left(\frac{\Gamma^2-1}{\Gamma^2}\times(u_x+v_y)-\frac{2\Phi}{3\Gamma^2}(p-r)\right)_0\right], \quad (20c)$$

$$\Gamma^2\delta q=\frac{k}{2}[(u_x-v_y-2q\Phi)^0+(u_x-v_y-2q\Phi)_0] \quad (20d)$$

$$\delta r=\frac{k}{2}\left[\left(\frac{\Gamma^2-2}{\Gamma^2}(u_x+v_y)-\frac{4\Phi}{3\Gamma^2}(r-p)\right)^0+\left(\frac{\Gamma^2-2}{\Gamma^2}\times(u_x+v_y)-\frac{4\Phi}{3\Gamma^2}(r-p)\right)_0\right], \quad (20e)$$

$$\Gamma^2\delta\tau=\frac{k}{2}[(u_y+v_x-2\tau\Phi)^0+(u_y+v_x-2\tau\Phi)_0]. \quad (20f)$$

All the terms on the right hand side of Eqs.(18) and Eqs.(20) can be evaluated from data on the plane $t=t_0-k$ except those terms having a superscript ^{0}. All the terms involving the unknown partial derivatives at 0 can be eliminated by forming linear combinations of Eqs. (20), and the eight equations obtained by writing Eqs.(18) for $\alpha_i=(i-1)\pi/2$, with $i=1, 2, 3, 4$.

In this way we obtain a system of six equation which determine the six unknown increments δu, δv, δp, δq, δr and $\delta\tau$. Also the following relations are used;

$$2ckw_x(x_0, y_0)=w(x_0+ck, y_0)-w(x_0-ck, y_0) \quad (21a)$$

$$(ck)^2w_{xx}(x_0, y_0)=w(x_0+ck, y_0)+w(x_0-ck, y_0)-2w(x_0, y_0) \quad (21b)$$

$$2ck^2w_{xy}(x_0, y_0)=k[w_x(x_0, y_0+ck)-w_x(x_0, y_0-ck)] \quad (21c)$$

$$0=k[w_x(x_0, y_0+ck)+w_x(x_0, y_0-ck)-2w_x(x_0, y_0)]. \quad (21d)$$

In Eqs.(21) c is equal to 1 for the exterior cones and to $1/\Gamma$ for the interior cones. The same relations hold if the roles of x and y in Eqs.(21) are changed. Just then six difference equations become

$$2\delta u=\frac{k^2}{\Gamma^2}\left[(\Gamma^2-1)v_{xy}+\Gamma^2u_{xx}+u_{yy}-2\left(\Phi\left(\frac{p-r}{3}+q\right)\right)_x-2(\Phi\tau)_y\right]_0+2k(q_x+p_x+\tau_y)_0, \quad (22a)$$

$$2\delta v=\frac{k^2}{\Gamma^2}\left[(\Gamma^2-1)u_{xy}+\Gamma^2v_{yy}+v_{xx}-2\left(\Phi\left(\frac{p-r}{3}-q\right)\right)_y-2(\Phi\tau)_x\right]_0+2k(p_y-q_y+\tau_x)_0, \quad (22b)$$

$$2\Gamma^2\delta\tau=-2k((\Phi\tau)^0+(\Phi\tau)_0)+k^2(2(p_{xy})_0+(\tau_{xx}+\tau_{yy})_0)-\frac{k^3}{\Gamma^2}((\Phi\tau)_{xx}+(\Phi\tau)_{yy})_0+2k(v_x+u_y)_0, \quad (22c)$$

$$2\Gamma^2\delta q=-\frac{k}{2}[4(\Phi q)^0+4(\Phi q)_0]-\frac{k^3}{\Gamma^2}\left[\left(\Phi\left(\frac{p-r}{3}+q\right)\right)_{xx}-\left(\Phi\left(\frac{p-r}{3}-q\right)\right)_{yy}\right]_0+2k(u_x-v_y)_0+k^2\times(q_{xx}+q_{yy}+p_{xx}-p_{yy})_0, \quad (22d)$$

$$2\frac{\Gamma^2}{\Gamma^2-1}\delta p=-\frac{k}{2}\left[\left(\frac{4\Phi(p-r)}{3(\Gamma^2-1)}\right)^0+\left(\frac{4\Phi(p-r)}{3(\Gamma^2-1)}\right)_0\right]+2k\times(u_x+v_y)_0-\frac{k^3}{\Gamma^2}\left[\left(\Phi\left(\frac{p-r}{3}+q\right)\right)_{xx}+\left(\Phi\frac{p-r}{3}-q\right)\right)_{yy}\Big]_0+k^2[q_{xx}-q_{yy}+p_{xx}+p_{yy}+2\tau_{xy}]_0, \quad (22e)$$

$$\delta r=\frac{\Gamma^2-2}{\Gamma^2-1}\delta p+\frac{k}{3\Gamma^2}\cdot\frac{3\Gamma^2-4}{\Gamma^2-1}[(\Phi(p-r))^0+(\Phi(p-r))_0]. \quad (22f)$$

The resulting difference scheme is a nine points scheme since the centered difference formulas for w_x, w_y, w_{xx}, w_{xy} and w_{yy} at (x_0, y_0) involve values for w at the mesh point (x_0, y_0) and the eight neighboring mesh points. Equations(22) are the difference equations at the points except the boundary points. Next the appropriate equations for mesh points on the boundary must be derived.

(a) Difference equations for mesh points on the boundary $y=0$, $|x|<1$

There equations are obtained by eliminating equations along bicharacteristics for which $\alpha=3\pi/2$ on both exterior and interior cones since these bicharacteristics intersect the plane $t=t_0-k$ at points outside the region of intersect. Combining Eqs.(18) and (20) as for interior points and then eliminating relations along the bicharacteristics corresponding to $\alpha=3\pi/2$ leads to the following equations for use at mesh points on the boundary $y=0$.

$$2\delta u=(22a)+(22c)/\Gamma, \quad (23a)$$

$$2\delta v+\frac{2\Gamma^2}{\Gamma^2-1}\delta p=(22b)+(22e), \quad (23b)$$

$$-2\delta v+2\Gamma^2\delta q=(22b)+(22d), \quad (23c)$$

$$\delta r=(22f). \quad (23d)$$

The terms on the right-hand side indicate the right-hand side of the corresponding equation of Eqs. (22). Equations (23) constitute four equations in six unknowns. The remaining two equations come from the boundary conditions on the boundary $y=0$. For the case being considered namely that of an applied normal pressure $P(x, t)$, the two additional equations are

$\tau(x, t)=0,$ (24a)

$p(x, t)-q(x, t)=P(x, t).$ (24b)

Then the following difference approximations are used. (These are the difference approximations in the case of $\lambda=k/h=0.5$)

$w_x=[w(x_0+h, y_0)-w(x_0-h, y_0)]/4h$ (25a)

$w_y=[w(x_0, y_0+h)-w(x_0, y_0)]/2h$ (25b)

$w_{xx}=[w(x_0+h, y_0)+w(x_0-h, y_0)-2w(x_0, y_0)]/2h^2$ (25c)

$w_{yy}=0$ (25d)

$w_{xy}=3[w(x_0+h, y_0+h)-w(x_0+h, y_0)-w(x_0-h, y_0+h)+w(x_0-h, y_0)]/4h^2$ (25e)

(b) Difference equations for mesh points on the boundary $|x|=1,\ y=0$

These equations are obtained by eliminating equations along bicharacteristics for which $\alpha=0,\ 3\pi/2$ on both exterior and interior cones. Thus the following equations are derived.

$\delta p-\delta q=\delta p(x, t),$ (26a)

$2\delta u+2\delta v-2\Gamma^2\delta q=$ (22a) − (22b) − (22d), (26b)

$-2\delta u+2\Gamma^2/(\Gamma^2-1)\delta p+2\delta v-2\Gamma\delta\tau$ = − (22a) + (22b) − (22c) $/\Gamma+$ (22e), (26c)

$\delta r=$ (22f). (26d)

And the two equations come from the boundary conditions. For example, when the material considered is bounded by stress-free boundaries,

$\delta p+\delta q=0,$ (26e)

$\delta\tau=0.$ (26f)

Then the following difference approximations are used.

$w_x=[w(x_0, 0)-w(x_0-h, 0)]/2h,$ (27a)

$w_y=[w(x_0, h)-w(x_0 h, 0)]/2h,$ (27b)

$w_{xx}=0,$ (27c)

$w_{yy}=0,$ (27d)

$w_{xy}=[w(x_0, h)+5w(x_0-h, 0)-5w(x_0, 0)-9w(x_0-h, h)]/8h^2$ (27e)

(c) Difference equations for mesh point on the boundary $|x|=1, 0<y<1$

These equations are obtained by eliminating equations along bicharacteristic for which $\alpha=0$ on both exterior and interior cones.

$2\delta u-2\Gamma^2/(\Gamma^2-1)\delta p=$ (22a) − (22b) (28a)

$2\delta v-2\Gamma\delta\tau=$ (22b) − (22c) $/\Gamma$ (28b)

$2\delta u-2\Gamma^2\delta b=$ (22a) − (22d) (28c)

$\delta r=$ (22f) (28d)

Form the boundary condition,

$\delta p+\delta q=0,$ (28e)

$\delta\tau=0.$ (28f)

Then the following difference approximations are used.

$w_x=[w(x_0, y_0)-w(x_0-h, y_0)]/2h$ (29a)

$w_y=[w(x_0, y_0+h)-w(x_0, y_0-h)]/4h,$ (29b)

$w_{xx}=0,$ (29c)

$w_{yy}=[w(x_0, y_0+h)+w(x_0, y_0-h)-2w(x_0, y_0)]/2h^2,$ (29d)

$w_{xy}=3[w(x_0, y_0+h)-w(x_0, y_0-h)+w(x_0-h, y_0-h)-w(x_0-h, y_0+h)]/4h^2$ (29e)

(d) Difference equations for mesh point on the boundary $|x|=1,\ y=1$

Eliminating equations along bicharacteristics for which $\alpha=0,\ \pi/2$ on both exterior and interior cones,

$2\delta u+2\delta v-\frac{2\Gamma^2}{\Gamma^2-1}\delta p-2\Gamma\delta\tau=$ (22a) + (22b) − (22e) − (22f) $/\Gamma,$ (30a)

$2\delta u-2\delta v-2\Gamma^2\delta q=$ (22a) − (22b) − (22d), (30b)

$\delta r=$ (22f). (30c)

From boundary condition,

$\delta u=0,$ (30d)

$\delta v=0,$ (30e)

$\delta p+\delta q=0.$ (30f)

Then the following difference approximations are used.

$w_x=[w(x_0, y_0)-w(x_0-h, y_0)]/2h,$ (31a)

$w_y=[w(x_0, y_0)-w(x_0, y_0-h)]/2h,$ (31b)

$w_{xx}=0,$ (31c)

$w_{yy}=0,$ (31d)

$w_{xy}=5[w(x_0-h, y_0-h)+w(x_0, y_0)-w(x_0, y_0-h)-w(x_0-h, y_0)]/8h^2$ (31e)

(e) Difference equations for mesh point on the boundary $|x|<1,\ y=1$

Eliminating equations along bicharacteristics for which $\alpha=\pi/2$ on both exterior and interior cones,

$2\delta v+2\Gamma^2\delta q=$ (22b) + (22d), (32a)

$2\delta u-2\Gamma\delta\tau=$ (22a) − (22c) $/\Gamma,$ (32b)

$2\delta v-2\Gamma^2/(\Gamma^2-1)\delta p=$ (22b) − (22e), (32c)

$\delta r=$ (22f). (32d)

From boundary conditions,

$\delta u=0,$ (32e)

$\delta v=0.$ (32f)

The following difference approximations are

$w_x=[w(x_0+h, y_0)-w(x_0-h, y_0)]/4h,$ (33a)

$w_y=[w(x_0, y_0)-w(x_0, y_0-h)]/2h,$ (33b)

$w_{xx}=[w(x_0+h, y_0)+w(x_0-h, y_0)-2w(x_0, y_0)]/2h^2,$ (33c)

$w_{yy}=0,$ (33d)

$w_{xy}=[w(x_0+h, y_0-h)-w(x_0+h, y_0)+w(x_0-h, y_0)-w(x_0-h, y_o-h)]/4h^2.$ (33e)

5. Numerical results and the consideration

For numerical calculations Eqs. (22), (23), (26), (28), (30) and (32) are used. In this paper the noninstantaneous plastic response term $\Phi(\bar{\sigma}, \bar{\varepsilon}_p)$ was assumed, in which $\Phi(\bar{\sigma}, \bar{\varepsilon}_p) = k(\bar{\sigma} - f(\bar{\varepsilon}_p))$, where k is a multiplicative constant and $f(\bar{\varepsilon}_p)$ is the equivelent strain in a quasi-static test.

The relation used for numerical calculations was

$$f(\bar{\varepsilon}_p) = A - \frac{B}{\bar{\sigma}/E + \bar{\varepsilon}_p}$$

The following data were used for aluminum;

$E = 7.031 \times 10^5$ kg/cm², $k = 10^6\ s^{-1}$,
$\rho = 0.28124 \times 10^{-5}$kg sec²/cm⁴, $\nu = 0.3$,
$G = 2.704 \times 10^5$ kg/cm²,
$A = 1406.2$kg/cm², $B = 0.7031$kg/cm²

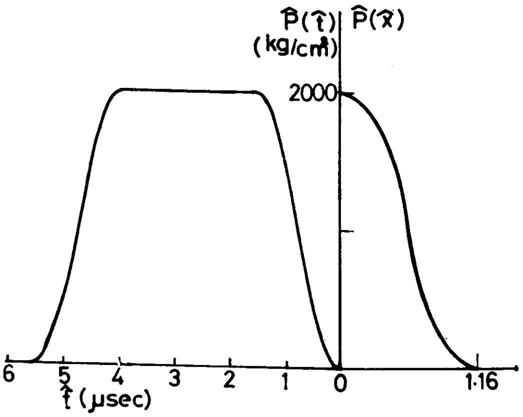

Fig. 3 Distribution of the pressure $\hat{P}(\hat{x}, \hat{t})$.

For these data we have

$c_1 = 580119$ cm/sec, $c_2 = 310086$cm/sec,
$\Gamma = c_1/c_2$.

The material considered is bounded by stress-free boundaries at $x = \pm 1$ and by stress-fix boundary at $y = 1$. For this example, we considered a symmetrical, continuous distribution of the pressure given by the relation (see Fig.3).

$0 \leqq x \leqq 1.16$cm : $\hat{P}(\hat{x}, \hat{t}) = \hat{P}_0(\cos(\pi\hat{x}/1.16) + 1)$ kg/cm²

$1.16 \leqq x \leqq 2.32$cm : $\hat{P}(\hat{x}, \hat{t}) = 0$.

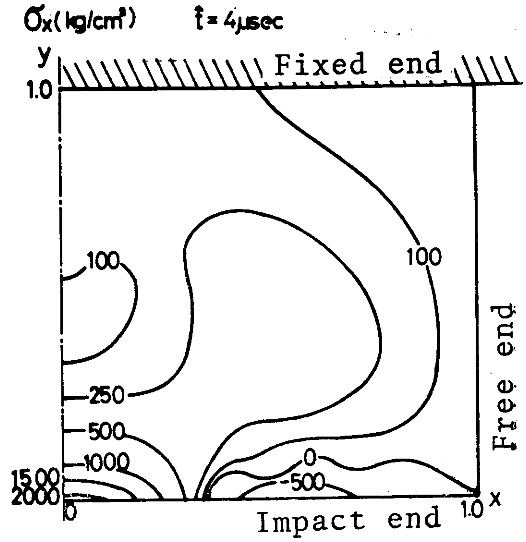

Fig. 5 Contour map of σ_x for $t = 4$ μsec.

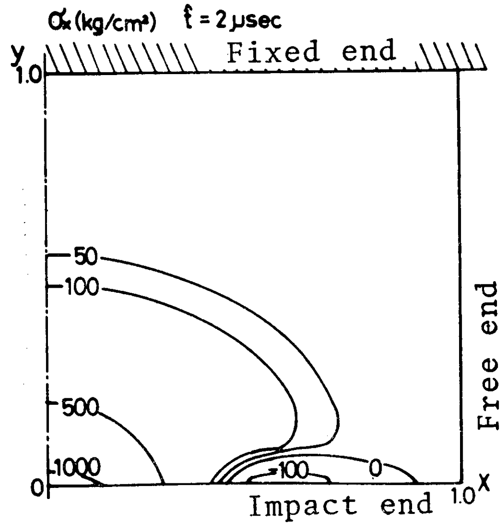

Fig. 4 Contour map of σ_x for $t = 2$ μsec.

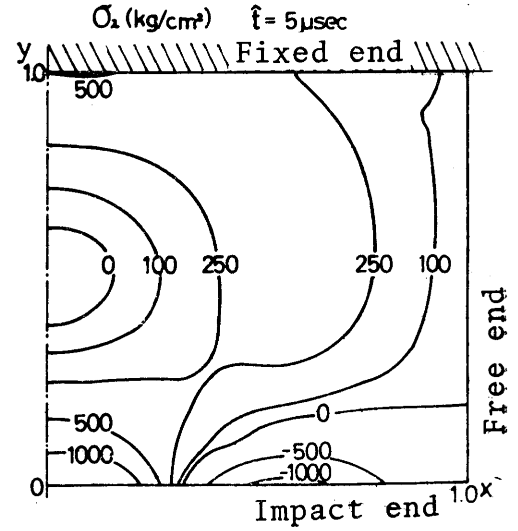

Fig. 6 Contour map of σ_x for $t = 5$ μsec.

An characteristic length b is set equal to 2.32 cm. We take the time interval $k=0.05$ and mesh dimension $h=0.1$. Thus $\lambda=k/h=0.5$, which is the value which assures the stability of difference equation.

The countor maps of each stress with time at $t=2, 4, 5$ μsec are shown in Figs. 4-12. The following fact is founded from Figs. 4-6; σ_x is propagated at the angle of about 45 deg. to $y=0$. It is because the propagation of the compressive stress to y direction applied on the impulsive face and the propagation of to x direction are superposed.

Unloading regions are produced near the center of symmetric surface and the unloading waves are propagated parallel to $y=0$. This phenomenon is produced because unloading waves comingf rom both stress-free boundaries are superposed on the symmetr ic surface and there unloading is accelerated.

The following face is founded from Figs. 7-9. At first σ_y is propagated to y direction and it spreads to x direction after it arrives at $y=1$. Figs. 10-12 show the fact that τ is propagated to y direction and that

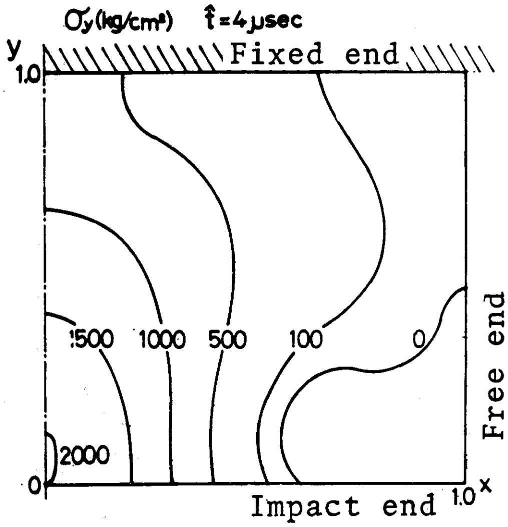

Fig. 7 Contour map of σ_y for $t=2$ μsec.

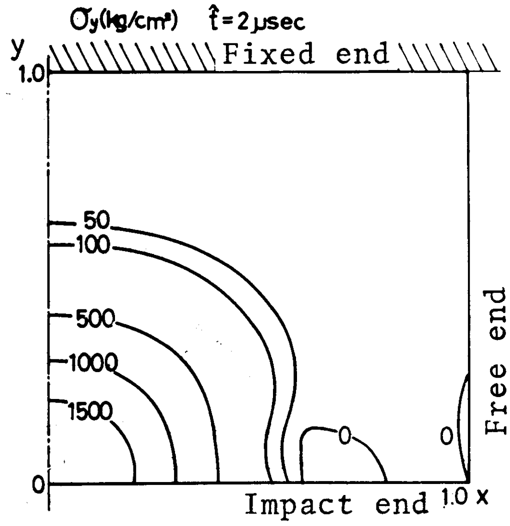

Fig. 8 Contour map of σ_y for $t=4$ μsec.

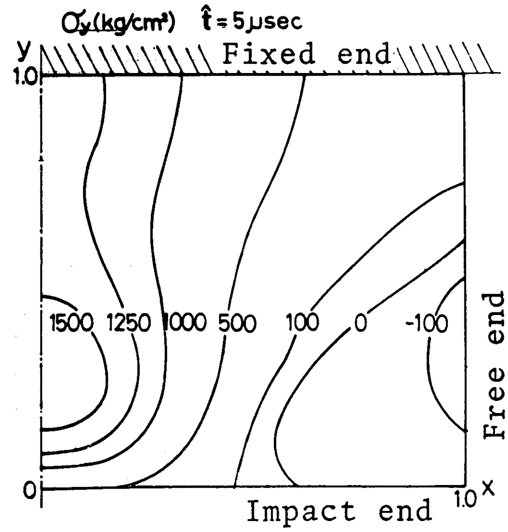

Fig. 9 Contour map of σ_y for $t=5$ μsec.

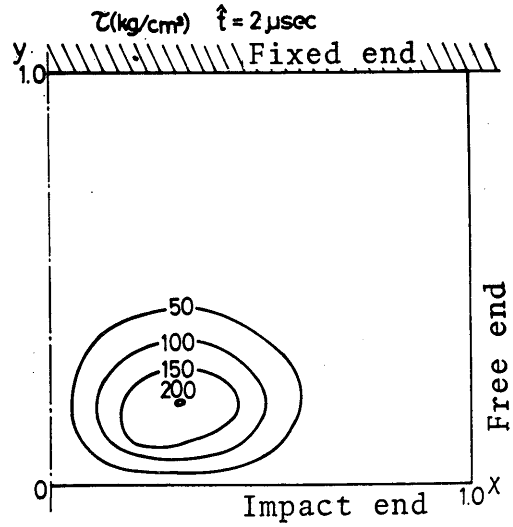

Fig. 10 Contour map of τ for $t=2$ μsec.

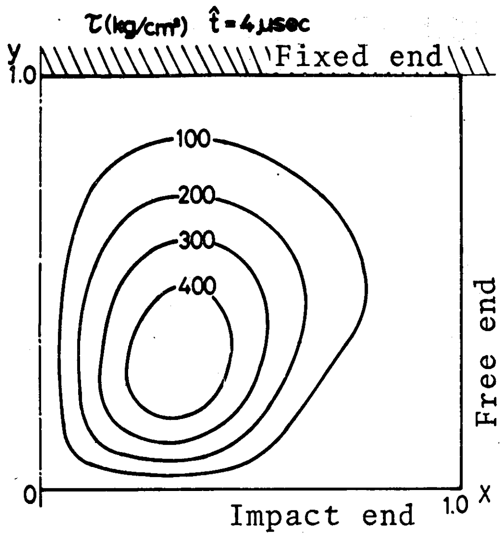

Fig.11 Contour map of τ for $t=4$ μsec.

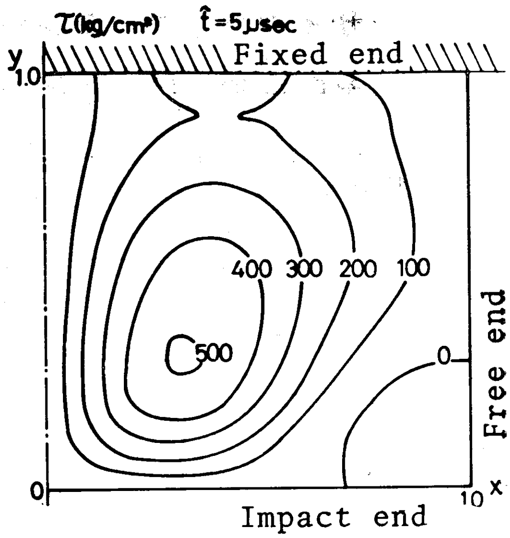

Fig.12 Contour map of τ for $t=5$ μsec.

the position where the maximum τ is produced hardly changes during the application of impulsive load.

6. Conclusion

From the contour maps of each stress, the following are concluded.

(1) Unloading regions are produced near the center of symmetric surface because of reflection of waves from the free boundaries. And then the unloading waves are propagated to x direction.

(2) The place where the shearing stress is the largest hardly changes during the application of impulsive load.

Acknowledgement

Thanks are due to Mr. S. Isogawa and H. Suizu for their assistance.

References

1) Bejda, J., Proc. Inter. Cong. appl. Mech., (1969), 121.
2) Malvern, L.E., Quart. appl. Math., 8 (1951), 405.
3) Malvern, L.E., J. appl. Mech., 18 (1951), 203.
4) Cristescu, N., Proc. Vibr. Probl., 6, 145.
5) Bleich, H.H. and Nelson, I., J. appl. Mech., 33 (1966), 149.
6) Ting, T.C.T. and Nan, N., J. appl. Mech. 36 (1969), 189.
7) Clifton, R.J., Proc. 5-th U.S.Nat. Cong. appl. Mech., (1966), 465.
8) Jeffery, A. and Taniuchi, T., Academi Press, New York, 1964.